Chapter 7

Comparison of the ^{1}H, ^{15}N, ^{13}C chemical shifts of the α-spectrin SH3 domain in solution and solid-state NMR

7.1 Introduction

A way to use the structural information contained in the chemical shift, is by investigating the differences of the chemical shifts in solution and solid-state[1,2]. These differences reflect changes in the direct environment of the system and should predominantly affect residues located at the surface of the molecule. A large perturbation in chemical shift can be due to several factors, such as changes in the molecular conformation, presence of local charges, ring-current effects arising from nearby aromatic groups or formation and disruption of hydrogen bonds.

In the case of the SH3 domain, the solid-state sample is in a micro-crystalline state, where, in extended highly-ordered domains, each SH3 molecule is in contact with other SH3 through well-defined contact areas. Differently, in a solution sample, the SH3 molecules are surrounded by water molecules. We used the crystal model obtained by x-ray diffraction[3] to explain the chemical shift differences in the solid-state and solution sample. Most of the differences are observed for residues located at the protein surface, that experiences the most drastic change of environment, i.e. from a water solution to contacts with other SH3 molecules.

7.2 Solution NMR assignment of the α-spectrin SH3 domain at pH = 7.5

The solid-state SH3 sample is prepared by precipitation of the protein from a water solution at pH = 7.5. To include the effect of the pH in the comparison of the solution and solid-state

chemical shifts, we have recorded and assigned solution data at pH = 7.5. At this pH, the SH3 molecules start to precipitate and therefore it is not possible to prepare a highly concentrated sample. The concentration of the sample we studied at this pH is low, < 0.15 mM, and it was not possible to obtain a complete assignment at this pH.

For the sequential resonance assignment of the SH3 domain at pH = 7.5, standard 3D triple-resonance experiments[4,5] on uniformly ^{13}C, ^{15}N-labelled samples were acquired. Most 3D triple-resonance experiments designed for proteins record $^{1}H^{N}$ and ^{15}N chemical shifts, in addition to a third frequency. 2D projections ($^{1}H^{N}/^{15}N$) of these spectra represent the usual ^{15}N-HSQC[6], which can be considered as the "fingerprint" of the protein, where each ($^{1}H^{N}$-^{15}N) peak corresponds to one residue. A HSQC spectrum of the SH3 domain at pH = 7.5 is shown in Fig. 7.1. Usually, the first 3D experiments to be recorded are of the type CBCA(CO)NH[7] and CBCANH[8], which connect ^{13}C chemical shifts of C^{α} and C^{β} to each ($^{1}H^{N}/^{15}N$) frequency pair. In particular in the CBCA(CO)NH experiment, the ($^{1}H^{N}/^{15}N$) frequency pair of each residue (i) is correlated with the C^{α} and C^{β} chemical shifts of the previous residue (i-1), while in the CBCANH experiment four peaks are detected, corresponding to the C^{α} and C^{β} chemical shifts of residues i and (i-1). By matching C^{α} and C^{β} chemical shifts of residues i and (i-1) in both spectra, neighbouring residues can be identified and linked up so that subsequences of residues are formed. These are then matched to the protein sequence. The C^{α} and C^{β} chemical shifts are used to obtain information about the amino-acid type. In particular, alanine, serine and threonine residues can be identified unambiguously because of their unique C^{α} and C^{β} chemical shifts.

To facilitate the sequential assignment, the CBCA(CO)NH and CBCANH experiments were complemented with 2D ^{1}H-^{15}N amino-acid-selective experiments for alanine (i, i+1), glycine (i, i+1) and alanine (i+1)[9,10]. In case of the alanine (i, i+1) and glycine (i, i+1) experiments, the ($^{1}H^{N}$-^{15}N) peak of alanines and glycines and of their sequential neighbours are detected, while in the alanine (i+1) experiment, the ($^{1}H^{N}$-^{15}N) peak of residues following alanines are recorded. Because of the presence in the SH3 sequence of two sequential alanines (A55 and A56), the ($^{1}H^{N}$-^{15}N) signal from A56 could be uniquely identified, being present in both alanine (i, i+1), and alanine (i+1) experiments. The identification of A56 was used as the starting point for the sequential assignment. The $^{1}H^{N}$, ^{15}N, C^{α} and C^{β} chemical shifts of almost all residues of the SH3 at pH = 7.5 could be assigned.

Once the sequential assignment of the ^{15}N-HSQC spectrum of the SH3 at pH =7.5 was achieved, a 3D triple-resonance experiment referred to as C(CO)NH-TOCSY was recorded, to complete the assignment of the ^{13}C side-chain resonances. In the third dimension of this 3D spectrum, the ^{13}C side-chain chemical shifts are detected, via a TOCSY-type transfer step[11,12]. In addition, the assignment of the carbonyl resonances was achieved by using a 3D HNCO experiment[4,13], where the ($^{1}H^{N}/^{15}N$) frequency pair of each residue (i) is correlated with the CO shift of residue (i-1). The assignment of the ^{1}H resonances was achieved by 3D triple-resonance experiments of the type HBHA(CO)NH and HC(CO)NH-TOCSY[5,14].

The chemical shifts at pH = 3.5 and pH = 7.5 are listed in Appendix A. The influence of the pH on most of the SH3 chemical shift values is very moderate. The only residues which show a significant change in the chemical shift are glutamic acids. In particular, the C^{β} and C^{γ} resonances of these amino-acids show a down-field shift of 1-3 ppm units, upon increasing the pH from 3.5 to 7.5. This can be readily explained by the fact that at higher pH, these acid residues become deprotonated.

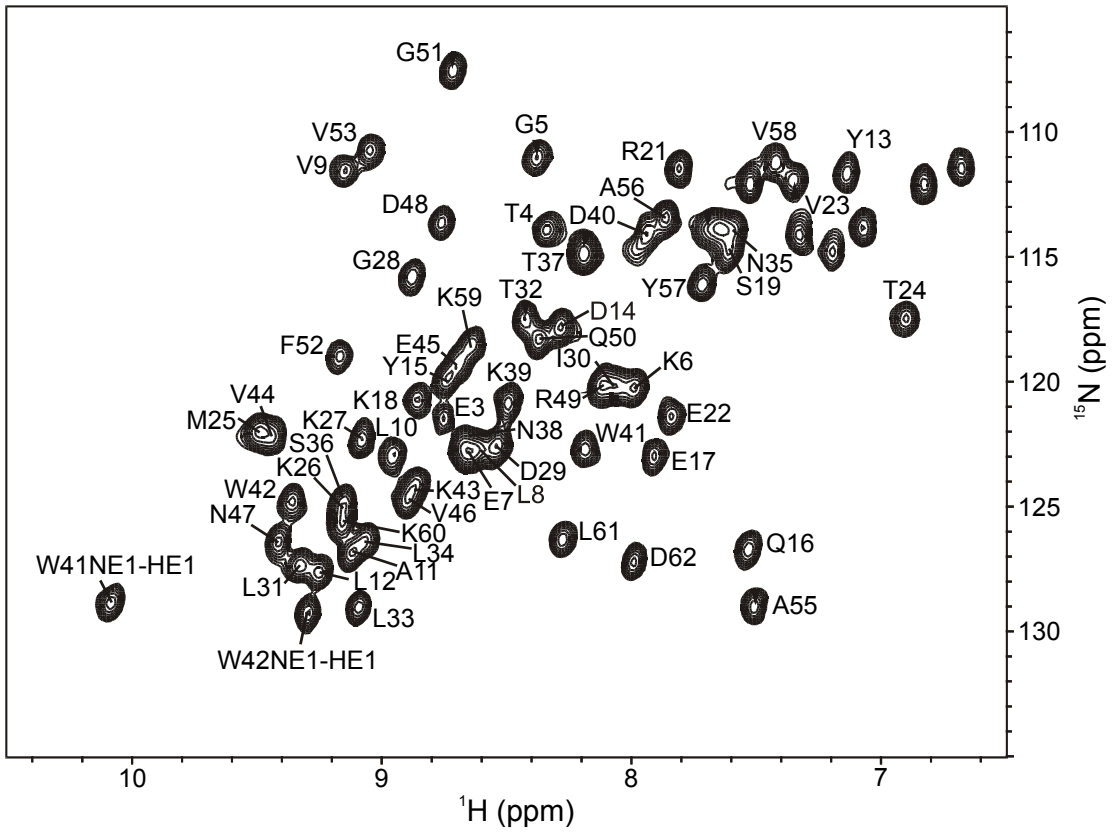

Fig. 7.1 ^{15}N-HSQC spectrum of the α-spectrin SH3 domain, at pH = 7.5. The spectrum is recorded at room temperature, at 9.4 T. The assignment is reported in the figure.

7.3 Chemical shift comparison in solution and solid-state NMR

In Appendix A, the ^{1}H, ^{13}C and ^{15}N chemical shifts of the α-spectrin SH3 domain in the solid-state are listed, together with the solution NMR shifts. From the table it can be seen that there is a remarkable similarity between the chemical shift values at the two sample conditions. Since chemical shifts are highly conformational dependent, this immediately indicates that the three dimensional fold of the protein in solution should be largely the same as in our micro-crystalline solid sample. The largest differences are observed for residues located at the protein surface, and can be explained by contacts with different SH3 molecules in the proximity. In the crystal model obtained by x-ray diffraction[3], a (P 21 21 21) crystal packing is defined, where each SH3 molecule has contacts with other molecules through three different contact areas. In Fig. 7.2, residues located in these three areas are colour-coded in red, blue and green. The same colour coding is used in Fig. 7.3, that shows correlation plots of the ^{1}H, ^{13}C and ^{15}N solid-state versus the liquid-state chemical shifts at pH= 7.5. From comparing Fig. 7.2 and Fig. 7.3 it can be seen that the main differences in ^{1}H, ^{13}C and ^{15}N chemical shift are indeed observed for nuclei of residues located in the contact areas.

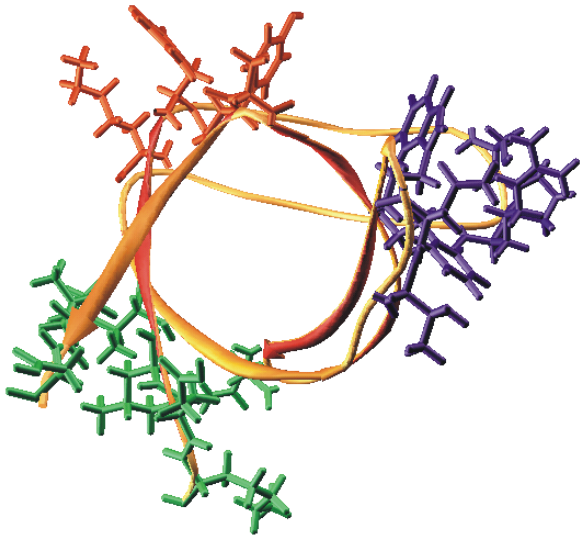

Fig. 7.2 3D structural model of the α-spectrin SH3 domain obtained by x-ray diffraction[3], completed with proton sites. The side-chains of residues in the three contact areas of the SH3 domain are shown, coloured in red, blue and green.

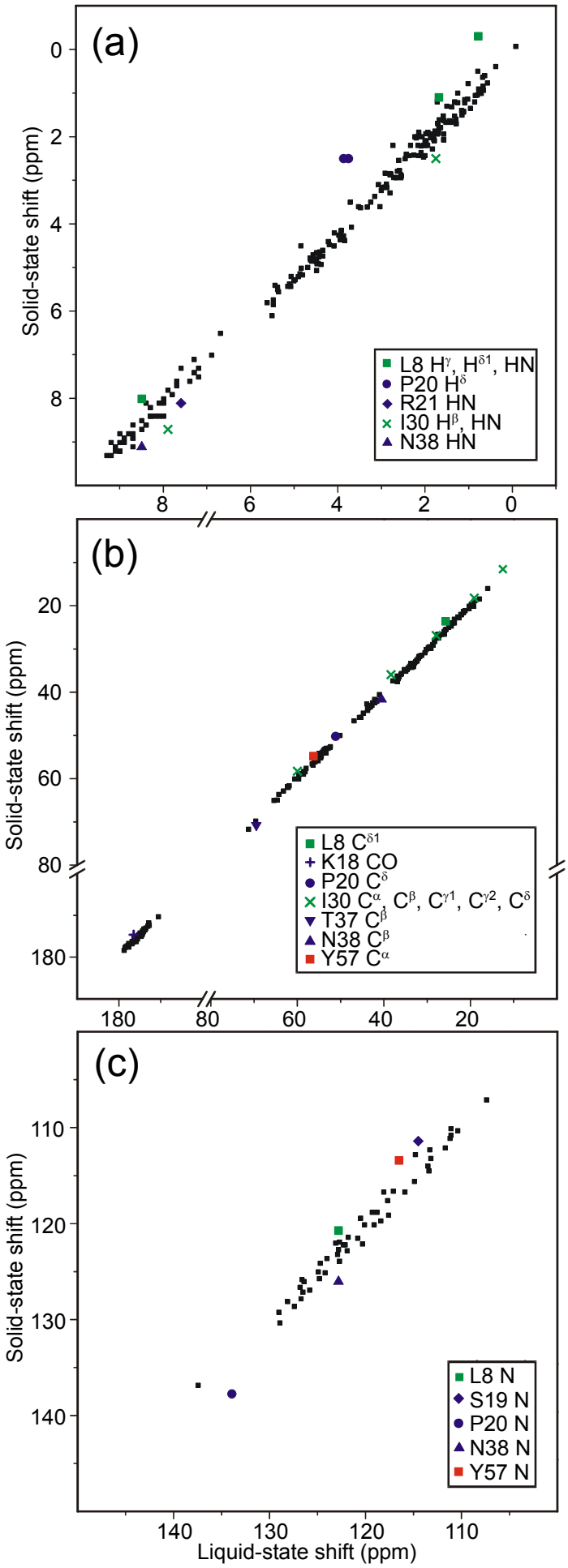
(a)
Solid-state shift (ppm)
0
2
4
6
8
8
6
4
2
0
L8 Hγ, Hδ1, HN
P20 Hδ
R21 HN
I30 Hβ, HN
N38 HN
(b)
Solid-state shift (ppm)
20
40
60
80
180
180
80
60
40
20
L8 Cδ1
K18 CO
P20 Cδ
I30 Cα, Cβ, Cγ1, Cγ2, Cδ
T37 Cβ
N38 Cβ
Y57 Cα
(c)
Solid-state shift (ppm)
110
120
130
140
140
130
120
110
Liquid-state shift (ppm)
L8 N
S19 N
P20 N
N38 N
Y57 N

Fig. 7.3 Correlation plots of the ^{1}H (a), ^{13}C (b) and ^{15}N (c) solid-state chemical shifts versus the liquid-state shifts at pH= 7.5. Nuclei with ^{1}H chemical shift differences larger that 0.5 ppm, ^{13}C chemical shift differences larger that 1.0 ppm and ^{15}N chemical shift differences larger that 2.0 ppm are indicated in the legend. The same colour coding is used as in Fig. 7.2.

In the correlation plot for the protons (Fig. 7.3a), the aliphatic and the amide protons are compared. The most significant shift differences are up-field shifts observed in the solid-state for L8 $H^{\delta 1}$ and P20 H^{δ}. Up-field shifts are also detected for the carbon nuclei L8 $C^{\delta 1}$ and P20 C^{δ} (Fig. 7.3b). The chemical shift of P20 C^{δ} is shifted relative to the shifts found in solution by −1.2 ppm, and the chemical shift of H^{δ} by −1.5 ppm. These shifts can be explained by the presence of two nearby aromatic rings from different SH3 molecules. In the structural model obtained by x-ray diffraction, this proline is located above the aromatic ring of Y13 from a neighboring SH3 domain, the C^{δ} at a distance of ~3.5 Å above the tyrosine ring and the two δ protons at about 3 Å, as shown in Fig. 7.4a. Based on computations of ring-current shifts for conjugated ring systems, upfield shifts of approximately −1.0 ppm and −1.5 ppm are estimated for the C^{δ} and H^{δ} in this configuration, respectively. This is well in agreement with the observed chemical shift differences. Likewise, pronounced upfield shifts are detected for L8, of −1.3 ppm for $H^{\delta 1}$, and of −2.2 ppm for $C^{\delta 1}$, relative to the liquid state. These shifts reflect the presence of the nearby phenyl ring of F52 of a second SH3 molecule according to the x-ray structure, as depicted in Fig. 7.4b.

Additional large shift changes are observed for the intermolecular contact between T37 and I30. The chemical shift of T37 C^{β} is shifted down-field by 1.5 ppm, as well as the chemical shift of I30 HN, by 0.8 ppm. The latter represents also the largest difference in chemical shift of all the amide protons. In the x-ray model, the side-chain OH group of T37 is located at 1.9 Å from the amide proton of I30 of a neighbouring molecule. The down-field shift can be well explained with the formation of an hydrogen bond between the side-chain OH and the backbone amide, as depicted in Fig. 7.5. The opposite situation (i.e. disruption of an intra-molecular H-bond in the solid-state) could explain the up-field shifts for both the backbone nitrogen and its amide proton of residue L8. In this case, an explanation could be that the hydrogen bond between the NH group of L8 and the OH side-chain group of D62 is broken and replaced with a new hydrogen bond between the NH_2 side-chain group of R21 and the backbone carboxyl group of L61.

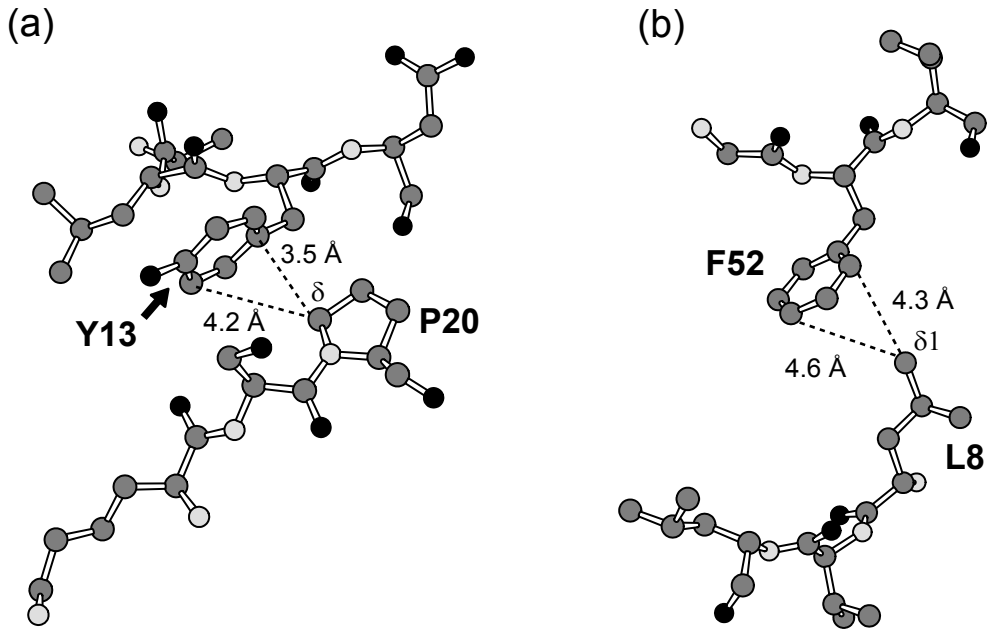

Fig. 7.4 Intermolecular contacts between side-chains from different SH3 domains according to the x-ray structure[3]. In particular, in (a) contact between P20 and Y13 and in (b)contact between L8 and F52.

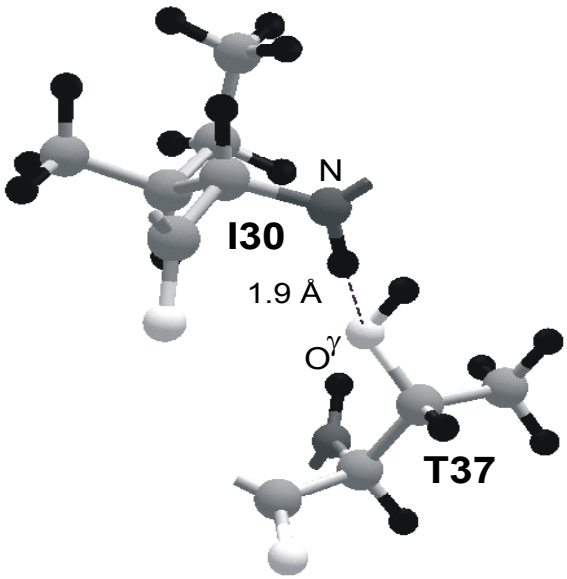

Fig. 7.5 Intermolecular contacts between different SH3 domains according to the x-ray structure[3]. The dotted line indicates the formation of an hydrogen bong between the side-chain OH group of T37 and the amide proton of I30.

There are still some changes which we were not able to interpret in terms of contacts between different SH3 molecules. An example is residue I30, for which the side-chain

carbons and the backbone α-carbon show a significant up-field shift of circa 1–2 ppm. In the x-ray model, the aromatic ring of F52 in a neighbouring SH3 molecule is located at 4–6 Å apart from I30. This distance is too big to explain the up-field shift. However, we believe that I30 is very flexible. This is derived from the fact that I30 signals are often inhomogeneously broadened. Furthermore, the ^{13}C magnetization exchange through the I30 side-chain was observed to be significantly slower than the exchange for other residue side-chains. A possible explanation of the change in chemical shift could be that this residue could spend part of the time in the proximity of the aromatic ring of F52. There are other changes in the backbone nitrogen chemical shifts, which are difficult to explain. Among those, the up-field shift of S19 N and the down-field shift of P20 N could be due to the formation of an hydrophobic pocket, formed by Y57 and Y13 from neighbouring SH3 molecules.

7.4 Conclusions

In summary, we exploited the information contained in the chemical shift by analysing the differences in the solution and in the solid-state NMR assignment. In the case of our micro-crystalline sample, some of the changes in the chemical shift values can be explained by ring-current effects, formation of hydrogen bonds between residues in neighbouring SH3 molecules or conformational changes due to disruption of H-bonds. Analysis of the chemical shift differences may be instrumental in ligand-receptor binding investigations, combining solution and solid-state NMR techniques. In this case, perturbations of the ligand resonances upon binding can be used to acquire structural insights of the binding interface.

7.5 Materials and methods

7.5.1 Solution NMR spectroscopy

For the solution NMR assignment at pH = 7.5, 3-4 mg of uniformly ^{13}C,^{15}N-labelled protein were first dissolved in a water solution at pH 3.5 and then the pH was raised to 7.5, by adding minute amounts of NaOH solution. At pH = 7.5, the protein started to precipitate, and the protein concentration in solution decreased to 0.15 mM. With time, we noticed the formation of additional precipitate on the bottom of the NMR tube, reducing the protein concentration even further. All solution NMR spectra were recorded at room temperature (300 K) on a

Bruker DRX-400 spectrometer operating at a proton frequency of 400.13 MHz, except the C(CO)NH-TOCSY experiment that was recorded on a Bruker DRX-600 spectrometer.

In the alanine (i, i+1), glycine (i, i+1) and alanine (i+1) selective experiments a multiplicity-selective coherence transfer step (MUSIC)[9,10] replaced the normal INEPT step in a HSQC pulse sequence. The ($^{1}H^{N}$-^{15}N) peaks of alanines and their following residues, the peaks of glycines and their following residues, and the sequential neighbours of alanines were detected, respectively. All 2D ^{1}H-^{15}N amino-acid-selective spectra were recorded with 44×384 complex points and spectral widths of 2000 Hz (^{15} N) × 6667 Hz (^{1}H). For the alanine (i, i+1) experiment, the total acquisition time was 15 hours, using 480 scans. For the glycine (i, i+1) experiment, the total acquisition time was 8 hours, using 256 scans. Finally, for the alanine (i+1) experiment, the total acquisition time was 4.5 hours, using 144 scans.

The 3D triple-resonance experiments of the type CBCA(CO)NH and CBCANH were recorded with 44×44×384 complex points and spectral widths of 6667 Hz (^{13}C) × 2000 Hz (^{15}N) × 6667 Hz (^{1}H). For the CBCA(CO)NH, the total acquisition time was 3 days and 16 hours, using 32 scans. For the CBCANH, the total acquisition time was 7 days and 8 hours, using 64 scans.

The 3D triple-resonance experiment of the type C(CO)NH-TOCSY was recorded with 64×56×512 complex points and spectral widths of 10000 Hz (^{13}C) × 3012 Hz (^{15}N) × 10000 Hz (^{1}H). The total acquisition time was 7 days and 7 hours, using 32 scans.

The 3D triple-resonance HNCO experiment was recorded with 44×44×384 complex points and spectral widths of 1667 Hz (^{13}C) × 2000 Hz (^{15}N) × 6667 Hz (^{1}H). The total acquisition time was 1 day and 20 hours, using 16 scans.

The 3D triple-resonance experiments of the type HBHA(CO)NH and HC(CO)NH-TOCSY were recorded with 41×41×384 complex points in each dimension and spectral widths of 2778 Hz (^{1}H) × 2000 Hz (^{15}N) × 6667 Hz (^{1}H). The total acquisition time for each 3D experiment was 6 days and 9 hours, using 64 scans.

All the solution data were processed were processed with the XWINNMR software, version 2.6 (Bruker, Karlsruhe, Germany) and subsequently analysed using the program Sparky, version 3.100 (T.D. Goddard & D.G. Kneller, University of California).

References

1. McDermott, A., Polenova, T., Bockmann, A., Zilm, K. W., Paulson, E. K., Martin, R. W., Montelione, G. T., & Paulsen, E. K. (2000). Partial NMR assignments for uniformly (13C, 15N)-enriched BPTI in the solid state. *J. Biomol. NMR* **16**, 209-219.

2. Williamson, P. T., Bains, S., Chung, C., Cooke, R., & Watts, A. (2002). Probing the environment of neurotensin whilst bound to the neurotensin receptor by solid state NMR. *FEBS Lett.* **518**, 111-115.

3. Musacchio, A., Noble, M., Pauptit, R., Wierenga, R., & Saraste, M. (1992). Crystal structure of a Src-homology 3 (SH3) domain. *Nature* **359**, 851-855.

4. Kay, L. E., Ikura, M., Tschudin, R., & Bax, A. (1990). 3-Dimensional Triple-Resonance Nmr-Spectroscopy of Isotopically Enriched Proteins. *J. Magn. Reson.* **89**, 496-514.

5. Montelione, G. T. & Wagner, G. (1990). Conformation-Independent Sequential Nmr Connections in Isotope-Enriched Polypeptides by H-1-C-13-N-15 Triple-Resonance Experiments. *J. Magn. Reson.* **87**, 183-188.

6. Sklenar, V., Piotto, M., Leppik, R., & Saudek, V. (1993). Gradient-Tailored Water Suppression for ^{1}H-^{15}N HSQC Experiments Optimized to Retain Full Sensitivity. *J. Magn. Reson. A* **102**, 241-245.

7. Grzesiek, S. & Bax, A. (1992). Correlating Backbone Amide and Side-Chain Resonances in Larger Proteins by Multiple Relayed Triple Resonance Nmr. *J. Am. Chem. Soc.* **114**, 6291-6293.

8. Grzesiek, S. & Bax, A. (1992). An Efficient Experiment for Sequential Backbone Assignment of Medium-Sized Isotopically Enriched Proteins. *J. Magn. Reson.* **99**, 201-207.

9. Schmieder, P., Leidert, M., Kelly, M., & Oschkinat, H. (1998). Multiplicity-Selective Coherence Transfer Steps for the Design of Amino Acid-Selective Experiments-A Triple-Resonance Experiment Selective for Asn and Gln. *J. Magn Reson.* **131**, 199-202.

10. Schubert, M., Smalla, M., Schmieder, P., & Oschkinat, H. (1999). MUSIC in triple-resonance experiments: amino acid type-selective (1)H-(15)N correlations. *J. Magn Reson.* **141**, 34-43.

11. Braunschweiler, L. & Ernst, R. R. (1983). Coherence Transfer by Isotropic Mixing - Application to Proton Correlation Spectroscopy. *J. Magn. Reson.* **53**, 521-528.

12. Bax, A. & Davis, D. G. (1985). Mlev-17-Based Two-Dimensional Homonuclear Magnetization Transfer Spectroscopy. *J. Magn. Reson.* **65**, 355-360.

13. Ikura, M., Kay, L. E., & Bax, A. (1990). A novel approach for sequential assignment of 1H, 13C, and 15N spectra of proteins: heteronuclear triple-resonance three-dimensional NMR spectroscopy. Application to calmodulin. *Biochemistry* **29**, 4659-4667.

14. Sattler, M., Schleucher, J., & Griesinger, C. (1999). Heteronuclear multidimensional NMR experiments for the structure determination of proteins in solution employing pulsed field gradients. *Prog. Nucl. Magn. Reson. Spectrosc.* **34**, 93-158.